Phase diagram for charge-density waves in a magnetic field

D. Zanchi
Laboratoire de Physique des Solides, associé au Centre National de la Recherche Scientifique, Université Paris-Sud, 91405 Orsay, France

A. Bjeliš
Department of Physics, Faculty of Science, University of Zagreb, POB 162, 41001 Zagreb, Croatia

G. Montambaux
Laboratoire de Physique des Solides, associé au Centre National de la Recherche Scientifique, Université Paris-Sud, 91405 Orsay, France

(Received 1 August 1995)

The influence of an external magnetic field on a quasi-one-dimensional system with a charge-density wave (CDW) instability is treated within the random-phase approximation which includes both CDW and spin-density wave correlations. We show that the CDW is sensitive to both orbital and Pauli effects of the field. In the case of perfect nesting, the critical temperature decreases monotonically with the field, and the wave vector of the instability starts to shift above some critical value of magnetic field. Depending on the ratio between the spin and charge coupling constants and on the direction of the applied magnetic field, the wave-vector shift is either parallel (CDW_x order) or perpendicular (CDW_y order) to the most conducting direction. The CDW_x order is a field-dependent linear combination of the charge- and spin-density waves and is sensible only to the Pauli effect. The wave-vector shift in CDW_y depends on the interchain coupling, but the critical temperature does not. This order is affected by the confinement of the electronic orbits. By increasing the relative strength of the orbital effect with respect to the Pauli effect, one can destroy the CDW_y, establishing either a CDW_x or a CDW_0 (corresponding to the perfect nesting wave vector). By increasing the imperfect nesting parameter, one passes from the regime where the critical temperature decreases with the field to the regime where it is initially enhanced by the orbital effect and eventually suppressed by the Pauli effect. For a bad nesting, the quantized phases of the field-induced CDW appear.

I. INTRODUCTION

The open and almost flat Fermi surface that characterizes the quasi-one-dimensional (Q1D) electronic systems gives rise to the formation of charge (or spin) density waves.[1–3] Moreover, the external magnetic field couples to the spin (via Pauli term) and to the orbits (via Peierls substitution in the Hamiltonian) of the electrons. This coupling affects the properties related to density wave (DW) formation like the order parameter, the critical temperature, and the wave vector of instability. The scale for the Pauli impact in the momentum space is the wave number $q_P=\mu_B H/v_F$, while the orbital effect enters through the inverse magnetic length $q_0=ebH\cos\theta$, where θ is the inclination of the magnetic field **H** from the transverse c direction in the (b,c) plane (a plane perpendicular to the chains). The ratio of these two characteristic wave numbers $\eta\equiv q_0/q_P=ebv_F\cos\theta/\mu_B$ is of the order of unity in real materials. It will play an important role in the phase diagram for the CDW in a magnetic field.

The Pauli term introduces a finite coupling between the CDW and the component of the SDW parallel to **H**, and may lead to a finite, magnetic-field-dependent, shift in the wave vector of instability.[4] It is therefore necessary to treat CDW and SDW together. A simple relevant model is the extended Hubbard or (g_1,g_2) model,[1,3] with coupling constants $U_s=g_2/2$ and $U_c=(2g_1-g_2)/2$ for the SDW and CDW, respectively. Since the Pauli term mixes the CDW with the SDW, the ratio $\nu\equiv -U_s/U_c$ will be the second relevant parameter for the CDW phase diagram.

The Pauli term breaks the rotational symmetry of the complex vectorial SDW order parameter, constraining its direction perpendicularly to magnetic field. With this constraint taken into account, the SDW phase diagram depends only on the orbital coupling, provided that the system is perfectly magnetically isotropic in the absence of magnetic field. However, the fluctuations of the component of SDW parallel to **H** around its zero value remain affected by both Pauli and orbital coupling. Moreover, the Pauli term introduces a finite coupling between these fluctuations and the noncritical CDW fluctuations.

The influence of a magnetic field on the CDW systems is even richer, because both Pauli and orbital effects can affect the CDW ordering. This fact is of direct experimental interest, since, e.g., the critical temperature can easily be measured. Furthermore, there is a finite magnetic field at which the wave vector of ordering starts to vary with the magnetic field. The description of these features, together with the interesting CDW-SDW mixing, is the main objective of the present detailed analysis.

The various aspects of the interaction between the electrons in Q1D systems and the external magnetic field have already been subjects of numerous analyses. The quadratic decrease of the mean-field critical temperature in one-dimensional CDW systems due to the Zeeman splitting was proposed theoretically,[5] and found experimentally in the organic compound TTF-TCNQ.[6] The recent very precise measurements in $Per_2[Au(mnt)_2]$ (Ref. 7) show the decrease of T_c which differs considerably from the theoretical value.[5]

The effect of the Pauli coupling on the CDW order parameter can be formulated as a breaking of degeneracy of two density waves, those with parallel and antiparallel spin with respect to **H**, each component being a CDW-SDW hybrid. This is reminiscent of the treatment of two coexisting CDW's with overlapping electronic bands.[8–10] The coupling of two CDW's with different wave vectors may stabilize a soliton lattice in the relative phase of two waves.[10]

On the other side, the orbital coupling alone leads to an increase of the critical temperature for CDW's.[11–13] Such an increase was observed in, e.g., $NbSe_3$.[14] The aim of the present work is to introduce both orbital and Pauli couplings, into the RPA calculation of the DW matrix susceptibility, and to determine some mean-field properties, in particular the phase diagram for CDW systems in a magnetic field.

In Sec. II we derive the RPA results for DW response functions in the form of a 4×4 matrix. In Sec. III we analyze in detail the phase diagram for CDW's in the case of a perfectly nested Fermi surface. In particular we consider the influence of the parameters ν, η and of the interchain hopping t_b on the critical temperature, the wave vector of the instability, and the CDW-SDW coupling. We also shortly discuss the effects of the imperfect nesting on the critical temperature as a function of magnetic field. The concluding remarks are given in Sec. IV.

II. MODEL

Quasi-one-dimensional electrons in an external magnetic field are usually modeled by the anisotropic two-dimensional Hamiltonian

$$\mathbf{H}_0=\frac{b}{2\pi}\int dq_y\int dx\Psi^\dagger(x,q_y)[H_{1D}+H_{Q1D,orb}+H_{Pauli}]\Psi(x,q_y) \tag{1}$$

with

$$H_{1D}=iv_F\rho_3\partial_x, \tag{2a}$$

$$H_{Q1D,orb}=2t_b\rho_3\ \sin(q_yb-q_0x)+2t_b'\ \cos2(q_yb-q_0x), \tag{2b}$$

$$H_{Pauli}=-\sigma_3\mu_BH. \tag{2c}$$

Here $\Psi^\dagger$ and Ψ are four-component fermion fields,

$$\Psi^\dagger=(\Psi^\dagger_{\uparrow+},\Psi^\dagger_{\uparrow-},\Psi^\dagger_{\downarrow+},\Psi^\dagger_{\downarrow-}),$$

where the indices $\uparrow,\downarrow$ span the spin space and σ_i are corresponding Pauli matrices. Indices $+(-)$ denote the right (left) Fermi surface with the states defined with respect to $\pm\mathbf{Q}/2$, where $\mathbf{Q}=(2k_F,\pi/b)$ is the wave vector of perfect nesting realized for $t_b'=0$, and ρ_i's are the Pauli matrices in that space. The chains lie in the xy plane and are parallel to the x axis. b is the lattice constant in the y direction. The longitudinal electronic dispersion given by H_{1D} is linearized in the vicinity of the Fermi wave numbers $\pm k_F$, with v_F being the longitudinal Fermi velocity. t_b is the hopping integral between nearest neighboring chains and t_b' parametrizes the imperfect nesting. The spin space is chosen to have the third component parallel to **H**.

Let us now introduce the relevant interaction part of the Hamiltonian. Since the further considerations are limited to the $2k_F$ RPA response, it is sufficient to keep only the contributions with bilinearly coupled electron-hole operators for spin- and charge-density waves. They are given by

$$\mathbf{H}_{int}=\int dx\sum_{\mathbf{R}_\perp}[-U_s\mathbf{M}^\dagger(\mathbf{R})\cdot\mathbf{M}(\mathbf{R})+U_cM_4^\dagger(\mathbf{R})M_4(\mathbf{R})]. \tag{3}$$

The two-fermion operators in Eq. (3) are defined by

$$M_i=\Psi^\dagger\rho_+\sigma_i\Psi,\quad i=1,2,3,4, \tag{4}$$

where $\sigma_4\equiv I$. The first three components ($i=1,2,3$) define the complex SDW vector amplitude **M**, while the fourth component M_4 is the complex CDW scalar amplitude. The SDW and CDW coupling constants in Eq. (3) are related to the usual backward (g_1) and forward (g_2) electron-electron coupling constants by $U_s\equiv g_2/2$ and $U_c\equiv(g_1-2g_2)/2$. We shall specify later the range of these constants for the most interesting physical cases relevant for our analysis.

The mean-field (MF) critical temperature for the spin- or charge-density wave is defined as the temperature at which the corresponding RPA susceptibility diverges. In our case the Pauli term introduces a finite coupling between the component of SDW parallel to the magnetic field (M_3) and the CDW (M_4). This coupling is appropriately treated by introducing the DW susceptibility matrix, with the elements defined as retarded correlators

$$\chi_{ij}(\mathbf{q},t-t')\equiv\langle M_iM_j^\dagger\rangle=-\theta(t-t')\langle[M_i(\mathbf{q},t),M_j^\dagger(\mathbf{q},t')]\rangle,\quad i,j=1,\ldots,4, \tag{5}$$

where $\mathbf{q}$ is the deviation of the wave vector from $(2k_F,\pi/b)$. The RPA result for this matrix is[4]

$$[\chi_{ij}(\mathbf{q},\omega)]=\begin{pmatrix}\frac{\chi_0(\mathbf{q},\omega)}{f^\perp} & 0 & 0 & 0\\ 0 & \frac{\chi_0(\mathbf{q},\omega)}{f^\perp} & 0 & 0\\ 0 & 0 & \frac{\chi_g(\sqrt{1+\delta^2}+U_c\chi_g)}{f^\parallel} & \frac{\chi_g\delta/f^\parallel}{}\\ 0 & 0 & \chi_g\delta/f^\parallel & \frac{\chi_g(\sqrt{1+\delta^2}-U_s\chi_g)}{f^\parallel}\end{pmatrix}, \tag{6}$$

with

$$\chi_g \equiv \sqrt{\chi_\uparrow(\mathbf{q},\omega)\chi_\downarrow(\mathbf{q},\omega)}, \tag{7a}$$

$$\chi_{\uparrow,\downarrow}(\mathbf{q},\omega_n) \equiv \chi_0(q_x \pm 2q_p, q_y, \omega_n), \tag{7b}$$

$$\delta \equiv [\chi_\uparrow(\mathbf{q},\omega) - \chi_\downarrow(\mathbf{q},\omega)]/2\chi_g, \tag{7c}$$

$$f^\parallel \equiv 1 + (U_c - U_s)\chi_g\sqrt{1+\delta^2} - U_c U_s \chi_g^2, \tag{7d}$$

$$f^\perp \equiv 1 - U_s \chi_0(\mathbf{q},\omega). \tag{7e}$$

$\chi_0(\mathbf{q},\omega)$ is the susceptibility which includes orbital contributions of a magnetic field,

$$\chi_0(\mathbf{q},\omega_n) = \sum_{l=-\infty}^{\infty} P(q_x - lq_o, \omega_n) I_l^2(q_y), \tag{8}$$

where $P(k - lq_0, \omega_n)$ is the one-dimensional bubble. The coefficients $I_l(q_y)$ bring in the orbital quantization due to the finite transverse dispersion (2b),[12,15]

$$I_l(q_y) = \sum_{l'} J_{l-2l'}\left(\frac{4t_b}{v_F q_0}\sin\frac{q_y b}{2}\right) J_{l'}\left(\frac{2t_b'}{v_F q_0}\cos q_y b\right), \tag{9}$$

where J_l are Bessel functions.

Even without further diagonalization of the matrix (6), it is evident that the critical temperatures for the condensation of density waves follow from the conditions

$$f^\perp(\mathbf{q}_\perp, T_c^\perp) = 0 \tag{10}$$

and

$$f^\parallel(\mathbf{q}_\parallel, T_c^\parallel) = 0, \tag{11}$$

where all functions have to be taken in the static ($\omega = 0$) limit. $T_c^\perp$ is the critical temperature for the SDW with the orientation of the spin perpendicular to **H**, i.e., for the degenerate components M_1 and M_2. $T_c^\parallel$ is the critical temperature for the hybrid of the CDW and the SDW with the spin parallel to **H**, i.e., of the coupled block (M_3, M_4) in the matrix $[\chi_{ij}(\mathbf{q}, \omega = 0)]$. The corresponding wave vectors $\mathbf{q}_\perp$ and $\mathbf{q}_\parallel$ of the ordering are those which maximize the respective critical temperatures $T_c^\perp$ and $T_c^\parallel$. The true critical temperature of the DW instability is equal to $\max\{T_c^\perp, T_c^\parallel\}$.

Having in mind real systems, it is appropriate to distinguish the most important situations realized for two characteristic interaction schemes. In the case of repulsive interactions ($U_s > 0, U_c > 0$), usually analyzed in terms of the Hubbard model ($U_s = U_c > 0$), the stable ordering following from (7) is the SDW one, determined by the condition (10). In other words, as far as the system possesses the internal magnetic isotropy, there is no effect of Pauli coupling on the ordering. Its spin is oriented perpendicularly to **H**, while the wave vector is given by $\mathbf{q}_\perp = \mathbf{0}$ in the case of the good nesting ($t_b' \ll T_c$), and may pass through the well-known cascade of phase transitions due to the orbital effects when the deviation from the good nesting is large enough ($t_b' \geqslant T_c$).[16–19]

In the case of predominant electron-phonon interaction ($U_c < 0, |U_c| > U_s \geqslant 0$) the system prefers the CDW ordering. As it is obvious from Eq. (6), the off-diagonal matrix elements vanish in the absence of a magnetic field. The instability condition (11) then reduces to $1 + U_c\chi_0 = 0$, and the ordering involves only the CDW component M_4. For finite magnetic fields the relation (11) contains contributions originating from both orbital and Pauli terms in the Hamiltonian (1) and (3). The former enters through the bubble susceptibility (8), while the latter introduces the CDW-SDW (i.e., M_4-M_3) hybridization measured through the parameter δ. As it is seen from Eq. (7), δ is finite if $q_x \neq 0$. More explicitly, after diagonalizing the $M_3 - M_4$ block of the matrix (6) the normal components of the "vector" (4) read

$$M_- = \frac{1}{N}[\delta M_3 + \Delta M_4], \quad M_+ = \frac{1}{N}[\delta M_4 - \Delta M_3], \tag{12}$$

with

$$N \equiv \sqrt{\delta^2 + \Delta^2}$$

and

$$\Delta \equiv \frac{1-\nu}{2}U\chi_g + \sqrt{\left(\frac{1-\nu}{2}U\chi_g\right)^2 + \delta^2},$$

while the corresponding diagonal susceptibilities are

$$\chi_\pm^{-1} = \chi_g^{-1}\left[\sqrt{1+\delta^2} - \frac{1+\nu}{2}U\chi_g \pm \sqrt{\left(\frac{1-\nu}{2}U\chi_g\right)^2 + \delta^2}\right]. \tag{13}$$

In these equations we have defined

$$U \equiv -U_c, \quad \nu \equiv U_s/U = -U_s/U_c \tag{14}$$

as a convenient parametrization of coupling constants for the problem of the CDW in the magnetic field. The value of ν depends on the interactions which participate in the Hamiltonian (1) and (3). The global phase diagram[1] at $H = 0$ in (ν, U) space is shown in Fig. 1, where the regime which we analyze is the upper half-plane ($U > 0$). The superconducting (SC) instability which is present in this diagram is ignored in our RPA approach. However, since we are interested in the the effects of magnetic field, this omission can be justified even in the case when for $H = 0$ the singlet SC state (SS in Fig. 1) is stable, i.e., when $\nu < -1/3$. Namely, the superconducting phase is suppressed by the orbital effect of a magnetic field. The critical field at which the critical temperature for the singlet SC state drops to zero is given by[20]

$$H_c^{SC} = \frac{16\pi^2 T_{sc}^2(U,\nu)}{7\sqrt{2}\zeta(3)\mu_B \eta t_b}, \tag{15}$$

where T_{sc} is the critical temperature for the singlet superconducting state in the absence of a magnetic field. Considering $(g_1 + g_2)$ as the corresponding effective coupling constant,[1] one easily finds that T_{sc} is related to the critical temperature for the charge-density wave at zero magnetic field, T_c^0, by

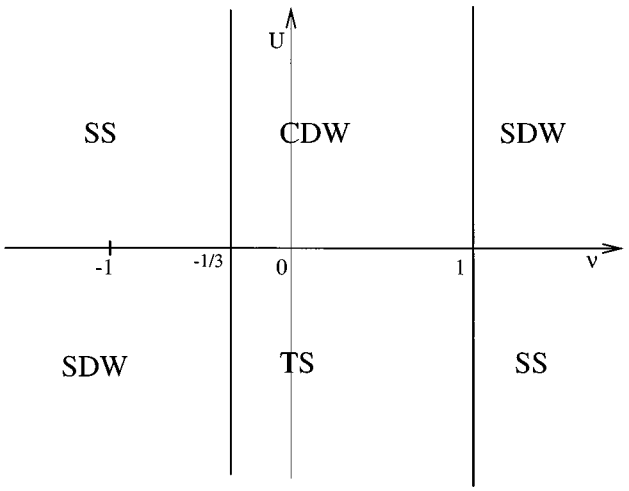

FIG. 1. A phase diagram of the one-dimensional system in the (ν,U) plane, in the absence of a magnetic field.

$$T_{sc}=T_c^0\,\exp\left[-\frac{\pi v_F}{U}\frac{1-3\nu}{1+3\nu}\right]. \tag{16}$$

Equations (15) and (16) give the estimation for the magnetic field above which our RPA results are valid even in the regime when the singlet superconductivity overwhelms the CDW.

It is useful for further discussion to mention here a few characteristic possibilities regarding the value of the parameter ν in the CDW (i.e., $U>0$) systems. Taking into account only pure backward electron-phonon interaction one has $\nu=0$. The inclusion of the presumably weaker repulsive Coulomb interaction between electrons shifts ν to some positive value. From the other side, a pure Hubbard model with attractive on-site interaction corresponds to $\nu=-1$. Altogether, ν covers a wide range of theoretically allowed values, but it should be noted that in the most frequent electron-phonon CDW systems this range is limited to $\nu\geqslant 0$.

Finally, it should be noted that the function $f^{\|}$ from the matrix (6) can be expressed in the factorized form, $f^{\|}=\chi_g^2\chi_-^{-1}\chi_+^{-1}$. Thus, for $U>0$ the condition (11) reduces to

$$\chi_-^{-1}(\mathbf{q},T_c)=0, \tag{17}$$

i.e., to the divergence of the susceptibility $\langle M_- M_-^{\dagger}\rangle$. Indeed, in the limit $\mathbf{H}\to\mathbf{0}$ the component M_- reduces to the pure CDW component M_4 and the divergence of χ_- coincides with the condition for the CDW instability, $1+U_c\chi_0=0$. Since the further discussion involves only the ordering with finite components M_3 and M_4, we simplify the notation for $T_c^{\|}$ and $\mathbf{q}_{\|}$ in Eq. (17) by skipping the index $\|$.

III. DISCUSSION

For $t_b'=0$, the wave vector of CDW ordering for $\mathbf{H}=\mathbf{0}$ is defined by the maximum of the susceptibility $\chi_0(\mathbf{q},\omega_n=0)$ (8) in the limit $q_0\to 0$. Of course it is located at $\mathbf{q}=\mathbf{0}$, i.e., at the wave vector of perfect nesting. The corresponding critical temperature $T_c^0=(2\gamma E_F/\pi)\exp(-\pi v_F/U)$ defines the temperature scale of the problem.

We want now to calculate the position of the minimum of χ_-^{-1} [Eq. (13)] in the momentum space. The criterion of local stability of the ordering with $\mathbf{q}=\mathbf{0}$ at finite $\mathbf{H}$ can be derived from the quadratic expansion of χ_-^{-1} with respect to q_x and q_y. For $T=T_c(H)$ it suffices to expand the [ ] bracket in Eq. (13). Noting that there is no bilinearly mixed term (q_xq_y), one gets

$$U^{-1}\chi_g\chi_-^{-1}\simeq U^{-1}-\chi_0+a_xq_x^2+a_yq_y^2+b_yq_y^4 +\mathcal{O}(q_x^2q_y^2,q_x^4,\ldots), \tag{18}$$

with

$$a_x=-\frac{1}{2}\frac{\partial^2\chi_0}{\partial q_x^2}+\left[\frac{1}{2\chi_0^2}(U^{-1}+\chi_0)-\frac{1}{(1-\nu)U^2\chi_0^3}\right]\left(\frac{\partial\chi_0}{\partial q_x}\right)^2, \tag{19}$$

$$a_y=-\frac{1}{2}\frac{\partial^2\chi_0}{\partial q_y^2}, \tag{20}$$

and

$$b_y=-\frac{1}{4!}\frac{\partial^4\chi_0}{\partial q_y^4}, \tag{21}$$

with the values of $\chi_0\equiv\chi_0(q_x,q_y,\omega_n=0)$ and its derivatives taken at $q_x=2q_p,q_y=0$. For the later purposes we include one $(\sim q_y^4)$ of the fourth-order terms in the expansion (18). Note that the expansion (18) is valid for $q_x<4\pi T_c^0/v_F,q_y<4\pi T_c^0/(t_bb)$.

The dependence of the critical temperature for the ordering at $\mathbf{q}=\mathbf{0}$ on the magnetic field follows from the equation

$$U\chi_0=1. \tag{22}$$

For small values of H this expression reduces to the known result for the suppression of the critical temperature due to the Pauli splitting of the electron band,[5]

$$T_c=T_c^0[1-7\zeta(3)(\mu_BH/2\pi T_c^0)^2]. \tag{23}$$

The dependence of the coefficients a_x, a_y, and b_y on the magnetic field follows straightforwardly from Eqs. (8) and (9). To this end we use the relation

$$P(q_x)=\frac{1}{\pi v_F}\left[\ln\frac{2\gamma E_F}{\pi T}-\mathrm{Re}\Psi\left(\frac{1}{2}+\frac{iv_Fq_x}{4\pi T}\right)+\mathrm{Re}\Psi\left(\frac{1}{2}\right)\right], \tag{24}$$

where Ψ denotes the digamma function, and expand the coefficients (9) (with $t_b'=0$) in terms of q_y up to the quartic contribution. Taking into account also Eq. (22) one gets at $T=T_c(H)$

$$a_x=\frac{1}{2\pi v_F}\left[\frac{\partial^2}{\partial q_x^2}\,\mathrm{Re}\Psi-\frac{2\nu U}{(1-\nu)\pi v_F}\left(\frac{\partial}{\partial q_x}\,\mathrm{Re}\Psi\right)^2\right]_{q_x=2q_P} \tag{25}$$

with $\Psi\equiv\Psi(\frac{1}{2}+iv_Fq_x/4\pi T)$, and

$$a_y = \frac{1}{\pi v_F}\left(\frac{t_b}{2\pi T_c \eta h}\right)^2 b^2 \alpha_y , \tag{26}$$

$$b_y = \frac{1}{\pi v_F}\left(\frac{t_b}{2\pi T_c \eta h}\right)^2 b^4 \left[\left(\frac{t_b}{2\pi T_c \eta h}\right)^2 \beta_y - \frac{1}{12}\alpha_y\right]. \tag{27}$$

The coefficients α_y and β_y in Eq. (27) are given by

$$\alpha_y \equiv \mathrm{Re}\Psi\left(\frac{1}{2} + ih(1+\eta/2)\right) + \mathrm{Re}\Psi\left(\frac{1}{2} + ih(1-\eta/2)\right) - 2\ \mathrm{Re}\Psi\left(\frac{1}{2} + ih\right) \tag{28}$$

and

$$\beta_y \equiv \frac{1}{4}\mathrm{Re}\Psi\left(\frac{1}{2} + ih(1+\eta)\right) + \frac{1}{4}\mathrm{Re}\Psi\left(\frac{1}{2} + ih(1-\eta)\right) - \frac{1}{2}\mathrm{Re}\Psi\left(\frac{1}{2} + ih(1+\eta/2)\right) - \frac{1}{2}\mathrm{Re}\Psi\left(\frac{1}{2} + ih(1-\eta/2)\right) + \frac{3}{2}\mathrm{Re}\Psi\left(\frac{1}{2} + ih\right), \tag{29}$$

respectively. Here we have introduced the dimensionless variable $h \equiv \mu_B H/2\pi T$. Note that the quantities a_x and a_y determine the longitudinal and transverse correlation lengths for CDW fluctuations ($\xi_x = U\sqrt{a_x}$ and $\xi_y = U\sqrt{a_y}$) when the temperature is close to T_c.

The wave vector of ordering stays at $\mathbf{q}=\mathbf{0}$ as far as the coefficients $a_x(h)$ and $a_y(h)$ are positive, and starts to move in the longitudinal or transverse direction when the former or later coefficient changes sign. As it is seen from Eqs. (25) and (26), the function $a_x(h)/a_x(h=0)$ contains the interaction parameters U/v_F and ν, while the function $a_y(h)/a_y(h=0)$ depends only on the ratio $\eta = q_0/q_p = eb v_F \cos\theta/\mu_B$ which measures the relative impact of the orbital and Pauli coupling on the CDW. Note that the parameter η can be easily changed by varying the angle θ between the direction of magnetic field and the c axis. Since the reasons for possible deviations of stable components q_x and q_y from zero are essentially different, it is appropriate to consider each case separately.

The longitudinal component of the CDW wave vector. The coefficient a_x changes its sign at the critical field $h_{cx} \equiv \mu_B H_{cx}/2\pi T$ shown in Fig. 2. For small values of ν this dependence is given by

$$h_{cx} \approx h_c^0\left(1 - 2.47\nu\frac{U}{\pi v_F}\right) \tag{30}$$

with $h_c^0 \equiv \mu_B H_c^0/(2\pi T) = 0.304$. As it is seen in Fig. 2, all curves $h_{cx}(\nu)$ pass through two common points, given by $\nu = 0, h_{cx} = 0.304$ and $\nu = 1, h_{cx} = 0$. At these points, h_{cx} does not depend on U. The first point ($\nu = 0$) corresponds to the CDW ordering with the SDW coupling equal to zero. In the second case ($\nu = 1$) the interactions in the CDW and SDW channels are of equal strengths and opposite signs, i.e., we are at the CDW-SDW boundary. There, the longitudinal splitting of the wave vector starts already at $h_{cx} = 0$. The change of sign of a_x at $h_{cx}(\nu, U)$ causes a second-order transition from the phase with $\mathbf{q} = \mathbf{0}$ named CDW_0, to a phase with $\mathbf{q} = (q_x(h), 0)$, named CDW_x. The dependence of the wave vector on the magnetic field is the solution of the equation $\partial\chi_-^{-1}/\partial q_x = 0$, and can be written in the form

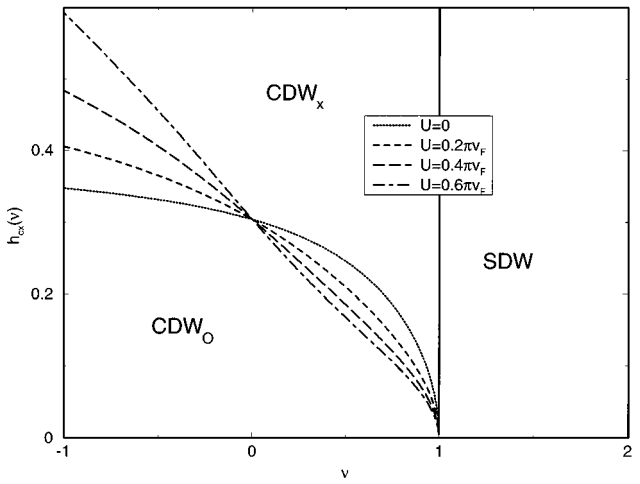

FIG. 2. Scaled critical magnetic field $h_{cx} \equiv \mu_B H_{cx}/(2\pi T)$ as a function of the parameter ν for few choices of the coupling constant: $U/\pi v_F = 0$, 0.2, 0.4, 0.6. Note that one has to insert $T_c(H)$ [and not $T_c(H=0)$] into the defining expression for h_{cx} in order to get a phase diagram with H dependence.

$$q_x = \frac{4\pi T}{v_F} f_{\nu,U}(h). \tag{31}$$

The function $f_{\nu,U}(h)$ is shown in Fig. 3 for $U/\pi v_F = 0.2$ and few values of ν. In the limit $h \gg 1$ one has $q_x(h) \to 2\mu_B H/v_F$, as it was already shown previously in the case of repulsive Hubbard model ($\nu = -1$).[4]

The transverse component of the CDW wave vector. The critical field h_{cy} at which a finite transverse component of the CDW vector develops is shown in Fig. 4. The line $h_{cy}(\eta)$ corresponds to the second-order transition from CDW_0 to a phase CDW_y with a transversely shifted wave vector. At small values of η the dependence $h_{cy}(\eta)$ is given by

$$h_{cy} \approx h_c^0\sqrt{1 + 0.088\eta^2}. \tag{32}$$

Here we use the approximative expression $\mathrm{Re}\Psi(\frac{1}{2} + ix) \approx \Psi(\frac{1}{2}) + 8.414x^2(1 + 3.81x^2)^{-1}$, valid for small values of the argument x. The dependence of the wave-vector component q_y on h for a fixed value of η can be represented by

$$q_y = \frac{2}{b}\arcsin\left[\frac{\pi T_c}{t_b} g_\eta(h)\right], \tag{33}$$

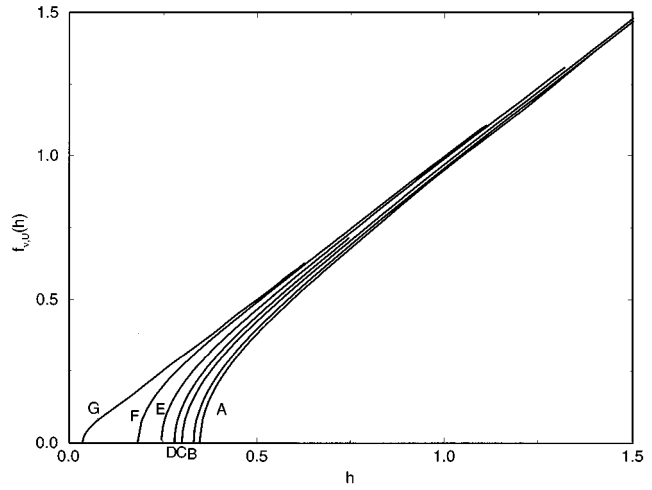

FIG. 3. The function $f_{\nu,U}(h)$, determining the dependence of the longitudinal shift of the wave vector on the magnetic field [see Eq. (31)], for $U/\pi v_F=0.2$ and $\nu=-1$ (A), -0.5 (B), 0.0 (C), 0.25 (D), 0.5 (E), 0.75 (F), 0.99 (G).

with the function $g_\eta(h)$ shown in Fig. 5. Note that unlike h_{cy} the wave-vector component q_y depends on t_b. For small values of $h-h_{cy}$ the function g_η reduces, after using Eq. (18), to

$$g_\eta(h)\approx 2\eta h\sqrt{-\frac{\alpha_y}{2\beta_y}}, \tag{34}$$

with α_y and β_y given by Eqs. (28) and (29), respectively. On the other hand, in the high-field limit $h\gg h_{cy}$ and for $\eta=0$ the function $g_{\eta=0}(h)$ is asymptotically given by $g_{\eta=0}(h\gg 1)\rightarrow h+\kappa$, where κ is of the order $1/\pi$. Note that the transverse shift of the wave vector does not depend on the interaction (ν or U). It depends, however, on η, i.e., on the relative impact of the Pauli and orbital effects. The reason for this is in the fact that all interaction dependence enters with δ [see Eq. (7)], which is equal to zero if $q_x=0$ and if the nesting is perfect. Thus, only a phase CDW_x is affected by the finiteness of the SDW coupling constant U_s (i.e., ν).

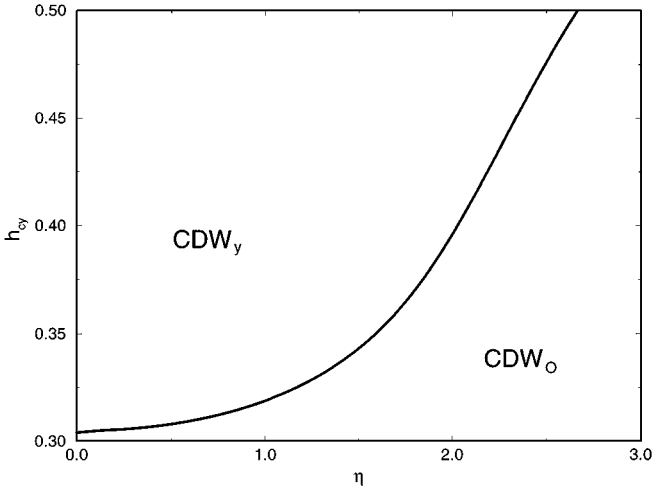

FIG. 4. Scaled critical magnetic field $h_{cy}\equiv\mu_B H_{cy}/(2\pi T)$ as a function of the parameter η.

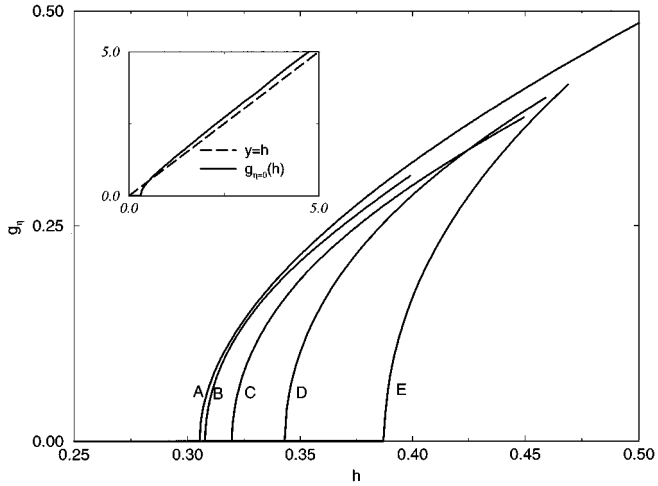

FIG. 5. A function $g_\eta(h)$, determining the dependence of the transverse shift of the wave vector on the magnetic field [see Eq. (33)], for $\eta=0$ (A), 0.5 (B), 1 (C), 1.5 (D), 2 (E). The inset shows the large x behavior for a case with no orbital effects ($\eta=0$).

The phase diagram for h larger than h_{cx} and/or h_{cy}. To provide some ideas on the variation of the wave vector of instability at magnetic fields larger than critical values h_{cx} and h_{cy}, it is useful to consider the symmetry and the shape of functions $\chi_0(\mathbf{q})$, $\chi_g(\mathbf{q})$, and $\chi_-^{-1}(\mathbf{q})$ at strong magnetic fields (h of order 1). Note first that all these functions are even in q_x and q_y. The function $\chi_0^{-1}(\mathbf{q})$ at $T\ll t_b$ has the line of local maxima given by[21]

$$q_x=\pm\left[\frac{4t_b}{v}\sin\frac{q_y b}{2}+\frac{1}{v}\mathcal{O}\left(\frac{T}{2t_b}\right)\right]. \tag{35}$$

When the Pauli term is introduced, the maxima of $\chi_\uparrow(\mathbf{q})$ will move to the left and those of $\chi_\downarrow(\mathbf{q})$ to the right by $2q_P$ along the axis q_x. The lines of local maxima of the susceptibilities χ_0, $\chi_\uparrow$, and $\chi_\downarrow$ are shown in Fig. 6(a). For h large enough the function $\chi_g(\mathbf{q})=\sqrt{\chi_\uparrow\chi_\downarrow}$, together with the function $-\chi_-^{-1}(\mathbf{q})$, will have two pairs of degenerate maxima in $\mathbf{q}$ space as candidates for absolute maxima. These two pairs have approximate positions at $(\pm 2q_P,0)$ and $(0,\pm(2/b)\arcsin(v_F q_P/2t_b))$ [denoted as A,A′ and B,B′, respectively, in Fig. 6(a)], in accord with the asymptotic limits given by Eqs. (31) and (33). In Fig. 6, we also show the function $-\chi_-^{-1}(\mathbf{q})$ for three characteristic choices of parameters ν, η, and U, i.e., when the absolute maxima are at $(0,\pm q_y)$ [Fig. 6(b)], at $(\pm 2q_P,0)$ [Fig. 6(c)], and when the two pairs of maxima have the same value [Fig. 6(d)]. As it was shown above, the phase transitions from the CDW_0 to CDW_x and CDW_y [Figs. 6(b) and 6(c)] are of the second order. The transition between the orderings CDW_x and CDW_y, caused by the competition of two maxima in $-\chi_-^{-1}(\mathbf{q})$ [Fig. 6(d)] is of the first order since the wave vector has a discontinuous jump between points $(q_x,0)$ and $(0,q_y)$ (i.e., between points A and B in Fig. 6).

To complete the phase diagram it is necessary to calculate

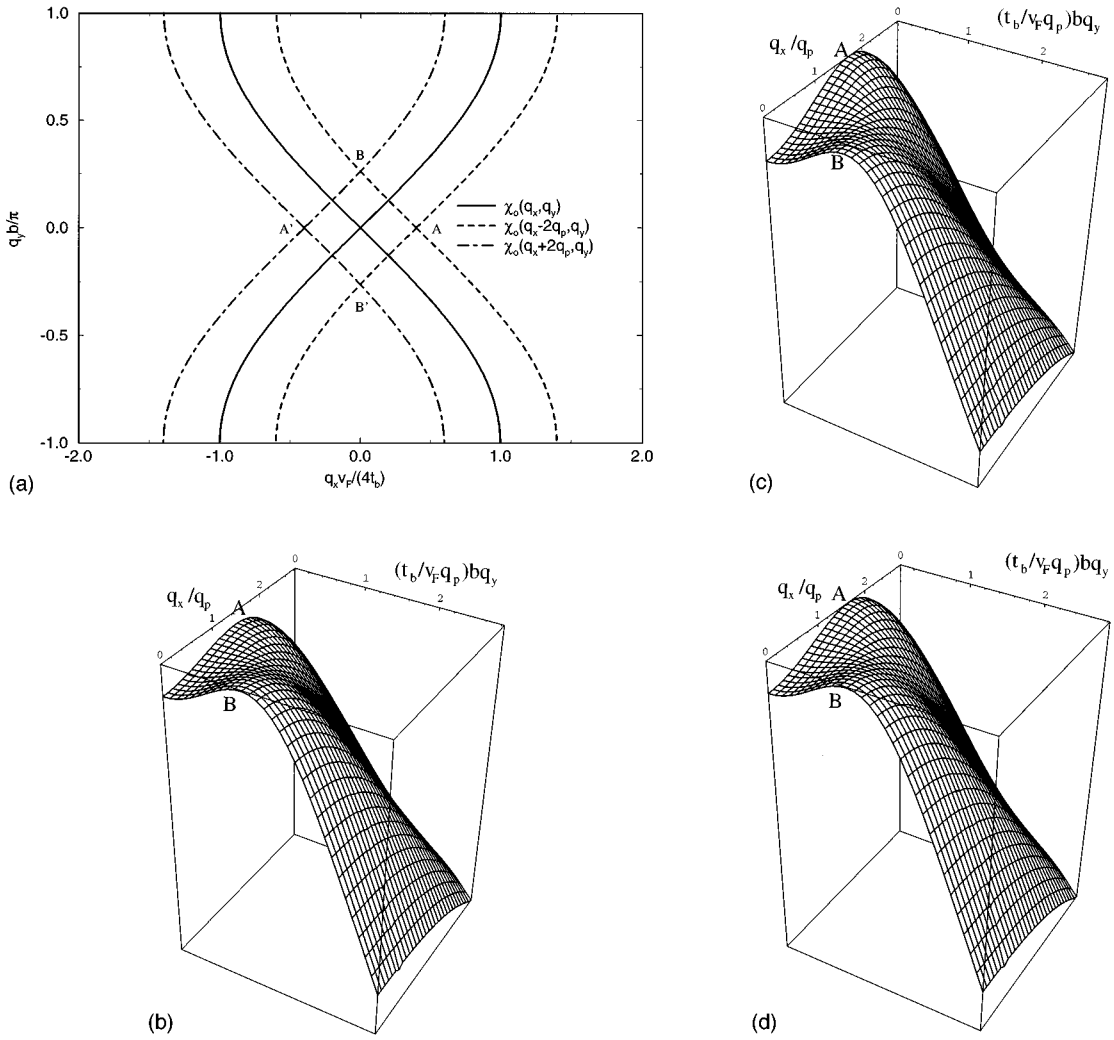

FIG. 6. (a) The lines of local maxima in $\mathbf{q}$ space of the susceptibility $\chi_0(q_x,q_y)$ (full line) without magnetic field, of $\chi_\uparrow \equiv \chi_0(q_x+2q_P,q_y)$ (dot-dashed line), and of $\chi_\downarrow \equiv \chi_0(q_x-2q_P,q_y)$ (dashed line). (A,A′) and (B,B′) are the two pairs of degenerate maxima of $\chi_g(q_x,q_y)$. (b), (c), and (d) show the function $-\chi_-^{-1}(\mathbf{q})$ at $T=0.42T_c^0$ and $\mu_B H=1.14T_c^0$, respectively, for three cases: $\nu=-1$ (CDW_y is stable, provided that the maxima are in the points B,B′), $\nu=-0.1$ (CDW_x is stable; the points A,A′ are dominant), and $\nu=-0.33$ (the first-order critical point between CDW_y and CDW_x, since all four points, A, A′, B, and B′ are of equal height).

the magnetic-field dependence of the critical temperatures, defined as the solutions of Eq. (5) for $\mathbf{q}=(0,0)$, $\mathbf{q}=(q_x,0)$, and $\mathbf{q}=(,q_y)$, and denoted by T_0, T_x, and T_y, respectively, and to determine $\max[T_0(H),T_x(H),T_y(H)]$. The dependence of critical temperatures T_0, T_x, and T_y on H for few values of ν and η and for $U/\pi v_F=0.2$ is shown in Fig. 7(a). The sections of lines $T_x(H)$ and $T_y(H)$ determine the critical magnetic fields and the temperatures of the first-order transitions. Note that the present analysis is based on the Landau expansion

$$F=\int d^2q\chi_-^{-1}(\mathbf{q})[M_-(\mathbf{q})M_-^*(\mathbf{q})]+\mathcal{O}(\{M_-^4\}), \quad (36)$$

which is restricted to the range of temperatures not far below $\max[T_0(H),T_x(H),T_y(H)]$.

Since the complete phase diagram depends on three parameters, H, ν, and η (with fixed U), it is appropriate to use two planes, (H,ν) (η being a parameter) and (H,η) (ν being a parameter), for its presentation, as shown in Figs. 7(b) and 7(c), respectively. We stress a particularly interesting situation $\nu\to 1^-$ for which the critical field h_{cx} goes to zero, and three phases (CDW_0, CDW_x, and SDW) are present in the narrow range of parameter ν. Note also the presence of the point in Figs. 7(b) and 7(c) at which the CDW_0, CDW_x, and CDW_y orders meet. The dependence $\nu(\eta)$ which defines this tricritical point is shown in Fig. 7(d). The corresponding magnetic field weakly varies with ν (i.e., η), as is seen in Figs. 7(b) and 7(c). The line in Fig. 7(d) thus divides the region where the wave vector shifts first in transversal direction from the region in which only a longitudinal shift is possible. Furthermore, among the CDW phases from Figs. 7(b) and 7(c) only the phase CDW_x has a finite fraction of the component M_3 [see Eq. (12)], and is thus a CDW-SDW hybrid. The ratio of components M_3 and M_4 follows from the constraint $M_+=0$. At $T=T_{cx}$ it is given by

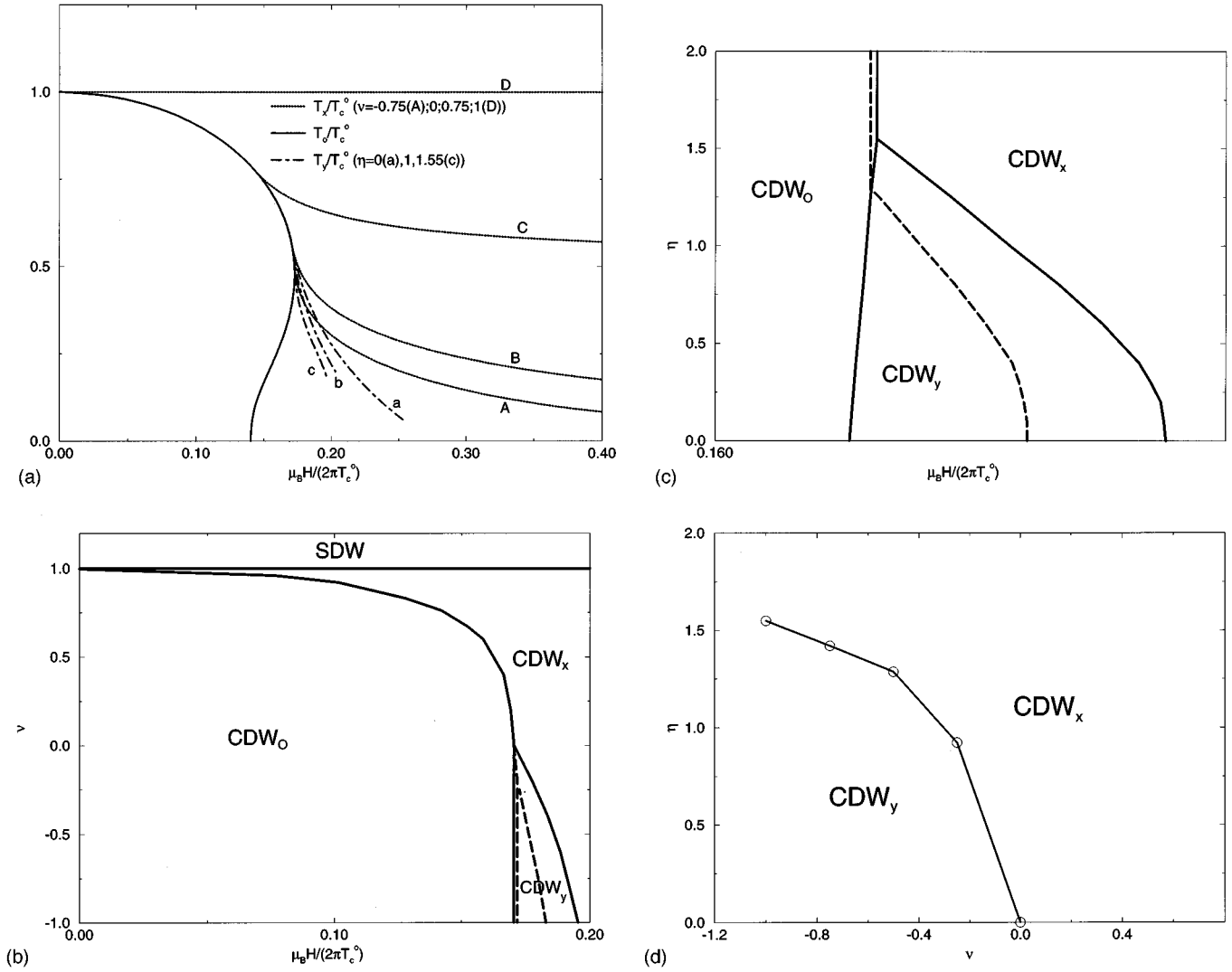

FIG. 7. (a) The critical temperatures T_0, T_x, and T_y for the CDW instabilities with the wave vectors $\mathbf{q}=\mathbf{0}$ (full line), $\mathbf{q}=(q_x,0)$ (dotted line), and $\mathbf{q}=(0,q_y)$ (dot-dashed line), respectively. For all curves $U/\pi v_F=0.2$. (b) The phase diagram in $(\nu,\mu BH/(2\pi T_c^0))$ plane for $\eta=0$. The changes of the diagram with finite η (here, $\eta=1$) are shown by dashed lines. (c) The phase diagram in $(\eta,\mu BH/(2\pi T_c^0))$ plane for $\nu=-1$. The changes of the diagram when $\nu=-0.5$ are dashed. (d) The curve in the (ν,η) plane which defines the tricritical point in (b) and (c).

$$M_3(\mathbf{q})=\frac{\delta(\mathbf{q})}{\sqrt{1+\delta^2(\mathbf{q})}-\nu U\chi_g(\mathbf{q})}M_4(\mathbf{q}), \tag{37}$$

and shown in Fig. 8 for few values of ν. Note that $|M_3/M_4|$ tends to 1 as one approaches the CDW_x–SDW transition.

Influence of the imperfect nesting. Let us finally consider a case when the imperfect nesting is introduced through a finite effective next-nearest-neighbor hopping t_b', which can be usually increased by, e.g., applying a strong pressure on a CDW system. For example, the relevant pressure scale in $NbSe_3$ is about 10 kbar.[12,23]

At small values of the magnetic field, the critical temperature for the phase CDW_0 can be readily found from the Eq. (22) yielding

$$T_c-T_c^0\approx-\left(\frac{\partial\chi_0}{\partial T}\right)\left[\frac{1}{2}\frac{\partial^2\chi_0}{\partial q_0^2}q_0^2-4a_xq_p^2\right]. \tag{38}$$

The values of $\partial\chi_0/\partial T$ and $\partial^2\chi_0/\partial q_0^2$ as functions of t_b' are given in Ref. 12. For small t_b', the coefficient a_x is given by

$$a_x\approx\frac{v_F}{32\pi^3T_c^0}\left[-\Psi''(1/2)+\Psi^{IV}(1/2)\left(\frac{t_b'}{2\pi T_c^0}\right)^2\right], \tag{39}$$

where $\Psi''\approx-16.83$ and $\Psi^{IV}\approx-771.47$. As one sees from Eq. (38), the orbital and Pauli effects are in competition, the former trying to enhance, and the latter to suppress T_c. For small $t_b'/T_c^0(t_b'=0)$ the function $\partial^2\chi_0/\partial q_0^2$ is proportional to $t_b'^2$. Moreover, the imperfect nesting decreases the coefficient a_x. Altogether, the general trend of the small t_b' is to flatten the H dependence of T_c.

For the sake of space, we present the result for the critical temperature which follows from Eq. (11) only for the case of attractive Hubbard interaction (i.e., $U/\pi v_F=0.2$, $\nu=-1$)

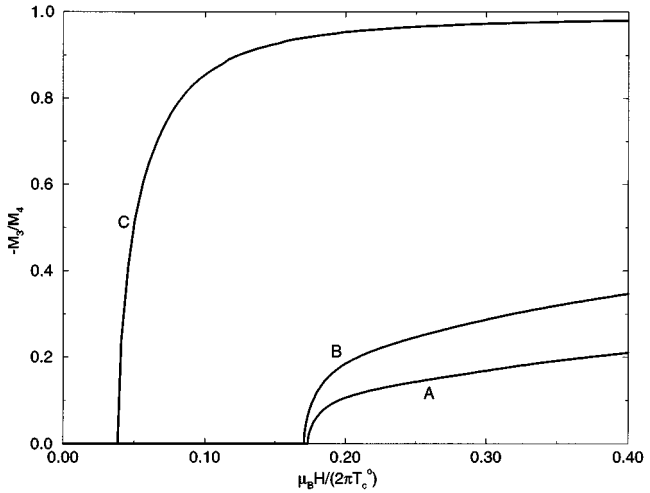

FIG. 8. The relative weight of the SDW and CDW components in the hybrid phase CDW_x as a function of magnetic field, for $U/\pi v_F=0.2$ and for $\nu=-1$ (A), 0 (B), 0.99 (C).

(Ref. 24) and for $\eta=2.5$. In this regime the orbital effects are strong enough, which excludes the stabilization of the CDW_y ordering when the nesting is good. The interplay between two effects of a magnetic field is a main characteristic of the phase diagram for imperfect nesting, given in Fig. 9. As the parameter t_b' increases from zero, the critical temperature only monotonously shifts to lower temperatures, still decreasing with a magnetic field. In other words, our results for the perfect nesting can be applied even to the systems with a moderate finite imperfect nesting, i.e., when the critical temperature remains far above the value of t_b'. The orbital effects enter manifestly into play at rather large values of t_b', enhancing the critical temperature initially, as it was observed in NbSe_3.[14] The eventual suppression of T_c by the Pauli term at high magnetic fields will make these diagrams basically different from the mean-field one for the FISDW with the orbital coupling only,[17] where no eventual suppression of the T_c is present. For a very bad nesting, i.e., for t_b' comparable to $t_b'^*$ [where $t_b'^*\sim T_c^0(t_b'=0)$ is the imperfect nesting parameter at which the CDW is destroyed at zero field[14]] the cyclotron frequency becomes the first relevant energy scale, giving the rise to a cascadelike shape, associated with the quantized field induced CDW phases. Notice that our approach does not explain the strong field breakdown of the high field phase in $(\mathrm{TMTSF})_2\mathrm{ClO}_4$,[22] since the Pauli term does not affect the SDW.

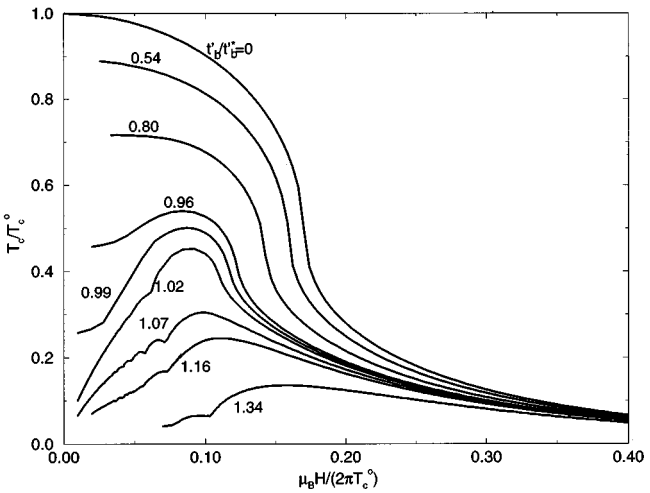

FIG. 9. The critical temperature vs magnetic field for a series of values of $t_b'/t_b'^*$ and for $U/\pi v_F=0.2$ and $\nu=-1$.

IV. CONCLUSION

The main result of the present work concerns the phase diagram of a CDW system in an external magnetic field. There are three physical parameters which characterize this diagram, namely the ratio of the SDW and CDW coupling constants, the strength of the magnetic field, and its direction with respect to the most conducting plane (x,y). The respective parameters are ν, h, and η. We recall that η also measures the relative impact of the orbital coupling with respect to the Pauli coupling.

In the case of a good nested Fermi surface the wave vector of the CDW has a general tendency to shift from its zero- field value $(2k_F,\pi/b)$ as the magnetic field increases [see Figs. 7(a)–7(c)]. This shift starts continuously, and may occur either longitudinally or transversally with respect to the chain direction. The longitudinal shift is governed solely by the Pauli coupling, with the corresponding CDW_x state being a hybrid of the pure CDW and of the SDW component parallel to the magnetic field. Both the critical value of the magnetic field h_{cx} at which q_x starts to shift, and the relative weights of the CDW and the SDW, depend on the ratio ν. Both $q_x(h)$ and the CDW-SDW hybridization increase with the magnetic field. It is important to mention that h_{cx}, q_x, and the hybridization ratio do not depend on t_b because all mean-field properties concerning a longitudinal tilt of the wave vector are given by pure one-dimensional expressions.

The shift of the CDW wave vector in the transverse direction is affected by both orbital and Pauli couplings. Contrary to the CDW_x, the CDW_y is not a CDW-SDW hybrid, and therefore is not influenced by the parameter ν. It exists only when t_b is finite, although the critical magnetic field h_{cy} does not depend on t_b. However, t_b influences the variation of q_y at $h>h_{cy}$, as shown by Eq. (33). $q_y(h)$ decreases with t_b and increases with the magnetic field. According to the general fact that the orbital effects lower the dimensionality of the electronic motion,[16] the effect of the increasing η is to favor the CDW_x. After some critical value of η (dependent on ν), the orbital impact reduces the phase diagram to the pure one-dimensional one, consisting only of the CDW_0 and CDW_x, as it is seen from Fig. 7(b).

At $\eta=0$ and for $\nu<0$, the shift of the wave vector is at first directed perpendicularly, and jumps to the longitudinal direction at some higher magnetic field. This jump between CDW_y and CDW_x is a first-order transition. On the contrary, for $0<\nu<1$, the wave vector is shifted longitudinally for all magnetic fields higher than the critical field $h_{cx}(\nu)$. Furthermore, $h_{cx}(\nu)$ tends to zero as ν approaches unity. The point $H=0,\nu=1$ is therefore tricritical, since $\nu>1$ is the range of SDW stability.

The Pauli and orbital terms together cause a rather complex magnetic-field dependence of the critical temperature in

systems with a finite imperfect nesting. This is illustrated in Fig. 9 in which t_b' varies from zero to the range above the critical value $t_b'^*$, at which the CDW ordering is completely eliminated at zero magnetic field. A rich dependence $T_c(H)$ contains the suppression by the Pauli term, enhancement by the orbital effects and, for large values of t_b', a cascadelike shape characterizing the field-induced DW. This phase diagram is quite general and not limited to the value $\nu=-1$, chosen in Fig. 9.

Our analysis for the perfect nesting case, showing a strong dependence of the critical properties in magnetic field on the ratio ν, could find an appropriate experimental support, e.g., in the MX compounds. The low-dimensional nature of these materials corresponds to our model. From our analysis, a particularly interesting possibility is that the Coulomb and electron-phonon forces can be tuned in a predictable manner by external pressure[25] or chemically,[26] allowing us to approach the phase boundary between CDW and SDW, corresponding to $\nu=1$. As we approach the boundary from the CDW side, the critical field for the $\mathrm{CDW}_0\rightarrow\mathrm{CDW}_x$ transition $h_{cx}\equiv H_{cx}/2\pi T$ will decrease rapidly toward zero, regardless of the value of $T\approx T_c$. Even for large T_c, by adjusting carefully ν, H_{cx} can decrease to experimentally reachable values, being extremely sensible to the variation of the parameter ν. We point out that a search for a magnetic-field-induced phase transitions in a CDW phase with strong SDW fluctuations (introduced by high pressure, for example) could confirm our predictions.

In $NbSe_3$ a phase transition in the 59 K CDW phase induced by magnetic field was found[27] by observing that a threshold electric field for the collective CDW motion is strongly reduced when magnetic field increases beyond the critical point. The naive explanation that this is a simple $\mathrm{CDW}_0\rightarrow\mathrm{CDW}_x$ one-dimension-like transition due only to the Pauli term must be taken with caution. Namely, the observed effect strongly depends on the angle θ, indicating that the orbital effects are also involved. This might mean that the strong orbital contributions, provided by a badly nested Fermi surface, affect the phase diagram. However, we believe that the Pauli term has an important role in this transition, since it enables the shift of the wave vector from its commensurable, perfect nesting position. We remind the reader that pure orbital effects can affect the wave vector only if it is not at the perfect nesting position [like in, e.g., $(TMTSF)_2ClO_4$ (Ref. 22)]. The fact that the nesting in $NbSe_3$ is quite bad can be deduced from a relatively strong pressure dependence of T_c ($dT_c/dP\approx-6.25$ K/KBr).[23] Indeed, from the comparison of a very weak enhancement of T_c with magnetic field[14] with our results in Fig. 9, it follows that the value of t_b' should be rather large.

Finally, our analysis of the imperfect nesting case can somewhat enlighten the recent measurements[7] in the compound $Per_2[Au(mnt)_2]$, where the suppression of the critical temperature proportional to the square of the magnetic field was found, but with a coefficient smaller than that which follows after taking only the Pauli coupling and a perfectly nested Fermi surface.[5] From Eq. (38) and from Fig. 9 one can conclude that the reason for the flattening of the suppression of T_c is just the finiteness of t_b'. However, the situation is not so simple. At finite values of t_b' the orbital effects come into play, in contrast to the experimental results which are independent on the field direction. If we just ignore the orbital effects, we get $t_b'\approx7.4$ K as an imperfect nesting parameter fitting the experimental curve. Finally, we indicate that the measurements of the critical properties in a magnetic field, and with pressure large enough to almost or completely destroy the zero-field CDW, could show very strong, cascadelike enhancement of the T_c for the quantized field induced CDW phases.

ACKNOWLEDGMENTS

We are indebted to S. Brazovskii, N. Dupuis, and J.-P. Pouget for inspiring discussions, and to M. Latković for the help in some of the numerical analyses.

[1] V. J. Emery, in *Highly Conducting One Dimensional Solids*, edited by J. T. Devreese, R. P. Evrard, and V. E. Van Doren (Plenum, New York, 1979), p. 247; J. Solyom, Adv. Phys. **28**, 201 (1979).

[2] *Electronic Properties of Inorganic Quasi-One-Dimensional Compounds*, edited by P. Monceau (Reidel, Dordrecht, 1985); *Low Dimensional Electronic Properties of Molybdenum Bronzes and Oxides*, edited by C. Schlenker (Kluwer, Dordrecht, 1989).

[3] D. Jérome and H. J. Schulz, Adv. Phys. **31**, 299 (1982).

[4] A. Bjeliš and D. Zanchi, Phys. Rev. B **49**, 5968 (1994).

[5] W. Dietrich and P. Fulde, Z. Phys. **265**, 239 (1973).

[6] T. Tiedje, J. F. Carolan, and A. J. Berlinsky, Can. J. Phys. **53**, 1593 (1975).

[7] G. Bonfait, M. J. Matos, R. T. Henriques, and M. Almeida, Physica B **211**, 297 (1995).

[8] S. A. Brazovskii and S. I. Matveenko, Zh. Eksp. Teor. Fiz. **87**, 1400 (1984) [Sov. Phys. JETP **60**, 804 (1984)].

[9] C. Noguera, J. Phys. C **19**, 2161 (1986).

[10] A. Bjeliš and S. Barišić, J. Phys. C **15**, 5607 (1986).

[11] C. A. Balseiro and L. M. Falicov, Phys. Rev. B **34**, 863 (1985).

[12] G. Montambaux, Phys. Rev. B **38**, 4788 (1988).

[13] A. Bjeliš and K. Maki, Phys. Rev. B **42**, 10 275 (1990).

[14] R. V. Coleman, M. P. Everson, H. A. Lu, and A. Johnson, Phys. Rev. B **41**, 460 (1990).

[15] A. Bjeliš and K. Maki, Phys. Rev. B **45**, 12 887 (1992).

[16] L. P. Gor'kov and A. G. Lebed, J. Phys. Lett. (Paris) **45**, L433 (1984).

[17] M. Héritier, G. Montambaux, and P. Lederer, J. Phys. Lett. **45**, L943 (1984).

[18] A. Virosztek, L. Chen, and K. Maki, Phys. Rev. B **34**, 3371 (1986).

[19] K. Yamaji, J. Phys. Soc. Jpn. **54**, 1034 (1985).

[20] N. Dupuis and G. Montambaux, Phys. Rev. B **49**, 8993 (1994).

[21] G. Montambaux, Ph.D. thesis, Université Paris–Sud, 1985.

[22] M. Naughton, R. V. Chamberlin, X. Yan, S.-Y. Hsu, L. Y. Chiang, M. Ya. Azbel, and P. M. Chaikin, Phys. Rev. Lett. **61**, 621 (1988).

[23] M. Núnéz Requeiro, J. M. Mignot, and D. Costello, Europhys. Lett. **18**, 53 (1992).

[24] $\nu=0$ actually corresponds to a stable SC phase. However, the form of the phase diagram is expected to be almost the same for all negative values of ν.

[25] G. S. Kanner, J. T. Gammel, S. P. Love, S. R. Johnson, B. Scott, and B. I. Swanson, Phys. Rev. B **50**, 18 682 (1994).

[26] See, for example, B. I. Swanson, R. J. Donohoe, L. A. Worl, A. D. F. Bulou, C. A. Arrington, J. T. Gammel, A. Saxene, and A. R. Bishop, Mol. Cryst. Liq. Cryst. **194**, 43 (1991), and references therein.

[27] P. Monceau and J. Richard, Phys. Rev. B **37**, 7982 (1988).